Joint Special Interest Group meeting between euspen and ASPE
Dimensional Accuracy and Surface Finish in Additive Manufacturing,
KU Leuven, BE, October 2017
www.euspen.eu

Investigation of complementary use of optical metrology and x-ray computed tomography for surface finish in laser powder bed fusion additive manufacturing

Jason C. Fox[1*], Felix Kim[1], Zachary Reese[2], Christopher Evans[2], John S. Taylor[2]

[1]*National Institute of Standards and Technology*
[2]*University of North Carolina at Charlotte*

**jason.fox@nist.gov*

Abstract
The development of additive manufacturing (AM) has allowed for increased complexity of designs over traditional manufacturing; however, increased design complexity leads to greater difficulties in post process finishing of the part surfaces. Additionally, uncertainty surrounding the quality of the complex as-built surfaces hinders wide scale adoption of AM. As such, a strong understanding of the as-built surface texture is required to help determine the quality of the resultant part. Complex geometries and internal surfaces create challenges for conventional surface finish metrology, but X-ray Computed Tomography (XCT) has emerged as a candidate since it does not require direct line of sight to the surface being measured. In this work, a comparison of XCT and optical measurements are performed on additively manufactured samples with two main goals: to determine the capability of XCT measurements as a tool for surface finish metrology and to determine if XCT measurements can provide insight into locations of overhangs and undercuts, which are difficult to identify and assess through conventional surface finish metrology and may have a drastic effect on part performance. Samples made from nickel alloy 625 and 17-4 stainless steel were built using a commercially available laser powder bed fusion (LPBF) system. Laser confocal and XCT measurements are performed on the samples and compared to each other and to scanning electron microscope (SEM) images of the parts. The results of this work support the premise that XCT provides useful information about the topography of a AM component. This can complement measurements made using optical methods such as confocal microscopy and also deliver results on porosity, undercuts, and internal surfaces where optical methods cannot reach. However, more work is required to relate XCT capabilities to the Fourier domains more commonly used to describe optical instruments and the associated ISO filter specifications.

Additive manufacturing; laser powder bed fusion; x-ray computed tomography; surface finish;

1. Introduction

Additive manufacturing (AM) has emerged as a key technology for production of high-value and complex parts that reduces time-to-market and cost to manufacture [1]. A key benefit to the AM process is the capability to create lattice structures and highly complex, topology optimized parts that reduce weight. Laser powder bed fusion (L-PBF) in particular has generated a great deal of interest due to the fine focusing optics, layer thicknesses of 20 µm to 100 µm, and the process space (beam powers and travel velocities) over which the system operates that allows for fine detail compared to other AM technologies [2]. Despite this advantage, however, a limiting factor affecting widespread adoption of AM is the as-built surface topography of finished parts. As part complexity increases, the ability to alter the surfaces through a secondary operation (i.e., machining or polishing), either in situ or ex situ, decreases [3]. Thus, improvements in the as-built surface texture has been cited as a key need [1].

Previous studies have focused on optimization of parameters specifically for surface texture as well as determining the effect of as-built surface texture on the resultant part properties. However, most AM literature has focused on the arithmetic mean roughness (*Ra*) [4], which provides little information as to the physical mechanisms creating features on the surface [5,6]. This, in turn, makes it difficult to develop the functional correlations between measured surface data and part performance (e.g., fracture, fatigue).

In addition to a stronger understanding of the as-built surface texture of AM parts, development of non-destructive evaluation (NDE) techniques such as x-ray computed tomography (XCT) for surface texture measurement is needed. Traditional surface metrology equipment often requires line of sight or adequate clearance to contact the surface with a stylus, which can be difficult to achieve given the highly complex AM geometries [7]. Kerckhofs et al. carried out an initial investigation on feasibility of studying surface roughness with XCT. They presented a high resolution XCT image at 1.5 µm/voxel resolution[8]. Townsend et al. presented a methodology to extract areal surface texture and compare with a focus variation microscopy measurement. The XCT acquisition setting provided 17.3 µm/voxel resolution [9]. Thompson et al. have also aligned the XCT data to conventional measurements (coherent scanning interferometry (CSI) and focus variation (FV) microscopy) and provided a comparison. Two different XCT systems were used which provided resolution of 5.7 µm/voxel and 5 µm/voxel respectively[10]. Additionally, Thompson et al. showed a comparison of confocal microscopy (CM), CSI, and FV to XCT data, achieving a resolution of 4.69 µm/voxel, and suggesting the integration of results to "improve understanding of the behaviour and performance of complex surface topography measurement" [11].

The purpose of this research is to investigate the complimentary use of optical metrology techniques and XCT with the primary focus being the benefit that the volumetric XCT data can provide when aligned with the data from conventional

surface metrology equipment. Samples made from 17-4 stainless steel (17-4SS) and Inconel 625 (IN625) are measured using a laser confocal microscope and XCT system. The data from the two systems is then aligned to pinpoint locations on the laser confocal microscope data close to near surface defects to provide more context on numerical analysis.

2. Methodology

Surface height measurements were acquired with a laser confocal microscope system (Zeiss LSM 800[1]). All measurements were performed with a 10x objective and 0.5x tube lens or a 20x objective lens. The former creates a lateral resolution of 1.25 µm and the latter creates a lateral resolution of 0.31 µm. Measurements were post-processed with Digital Surf's ConfoMap software to remove outliers and level the surfaces. No other filtering was applied to the data.

X-ray Computed Tomography (XCT) scans were acquired with North Star Imaging (NSI) CXMM 50 metrological CT system. The system is equipped with a 225-kV reflection source including a tungsten target, a rotary stage, and a flat panel detector (127 µm/pixel) (Figure 1). A source voltage of 160 kV and current of 80 µA was used. A copper filter (4 mm-thick) was applied to reduce the effect of characteristic X-ray peaks as simulated by TASMICS software (Figure 2) [12]. The average X-ray energy was predicted as 110 keV, which was sufficient to penetrate the 5 mm × 5 mm sample dimension of Inconel 625. The sample was mounted on a plastic sample holder instead of a metal one to reduce potential scattering effect from metal. The voxel size of the XCT data was calibrated based on a calibration object as 10.9 µm for a geometric magnification of 11.65 in each direction. A typical filtered backprojection algorithm supplied by the vendor was used to reconstruct the dataset [13]. XCT acquisition parameters are shown in Table 1.

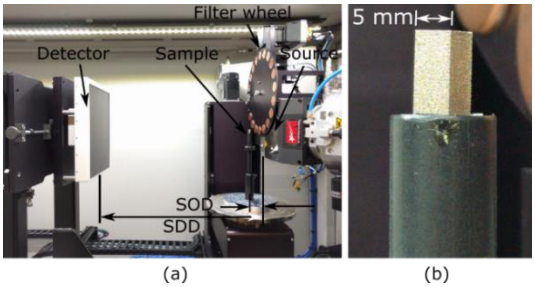

Figure 1. (a) XCT system setup, and (b) an example image of the sample

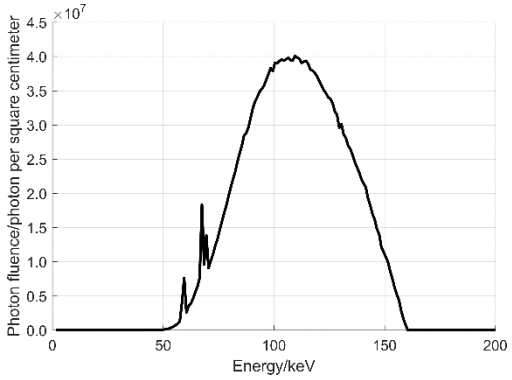

Figure 2. Simulated X-ray spectrum of 160 kV and 4 mm-thick copper filter for an air Kerma of 1 mGy.

Table 1. XCT acquisition parameters

Parameter	Value
Voltage	160 kV
Current	80 µA
Exposure time	2 s
Filter material/thickness	Cu/4 mm
Number of projection	1000
Source-to-detector distance (SDD)	492.76 mm
Source-to-object distance (SOD)	42.29 mm
Voxel size	10.9 µm

Parts for the analysis were built on the EOS M270 system at the National Institute of Standards and Technology (NIST). Three parts were built for this analysis: two using the commercially available EOS StainlessSteel GP1 (corresponds to US classification 17-4SS [14]) and one EOS NickelAlloy IN625 (corresponds to classification unified numbering system UNS N06625 [15]). It should be noted that the material used for the build was powder reclaimed from prior builds using an 80 µm sieve. It is assumed that the condition of the powder can have a large effect on the surface quality of parts being built and analysis of the powder is currently underway.

For the two parts built using the 17-4SS, the first was built entirely with the default parameters defined by the manufacturer, which will be referred to as "sample 60". The second was built with a beam power of 195 W and beam travel speed of 700 mm/s for the contour passes only (outermost portion of the part) with the rest of the parameters set to the default defined by the manufacturer and will be referred to as "sample 195". This high power contour setting was chosen because prior work by the authors had shown that these settings create a greater variety of surface features [6]. The part built using the IN625 was built with the default parameters defined by the manufacturer and will be referred to as "sample 625". Samples built for the analysis are shown in Figure 3.

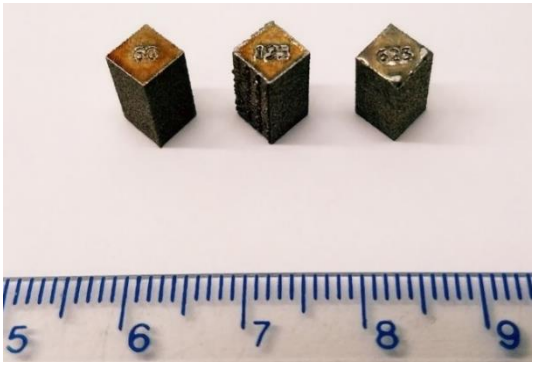

Figure 3. Sample 60 (left), sample 195 (center), and sample 625 (right). Scale is in mm.

The samples were built with the same orientation in the build chamber relative to the recoater blade. Surfaces of the samples will be referred to as follows: the top surface is parallel with the build plane and contains the part labels "60", "195", and "625", seen in Figure 3. Side surfaces will be referred to using primary intercardinal directions when looking down at the label on the top surfaces. For example, in Figure 3, the southeast (SE) and southwest (SW) surfaces of each part can be seen and the northeast (NE) and northwest (NW) surfaces cannot be seen.

[1] Certain commercial entities, equipment, or materials may be identified in this document in order to describe an experimental procedure or concept adequately. Such identification is not intended to imply recommendation or endorsement by the National Institute of Standards and Technology, nor is it intended to imply that the entities, materials, or equipment are necessarily the best available for the purpose.

3. Experiment Results

3.1. Analysis of optical metrology data

Height measurements were taken from the surfaces of the samples using a laser confocal microscope. Each surface was scanned over a 5 x 5 stitch using a 10x objective and 0.5x tube lens to create a 5.89 mm x 5.89 mm view of the surface with 1.25 µm point spacing. An example data set, leveled and outliers removed using the commercially available ConfoMap software, can be seen in Figure 4.

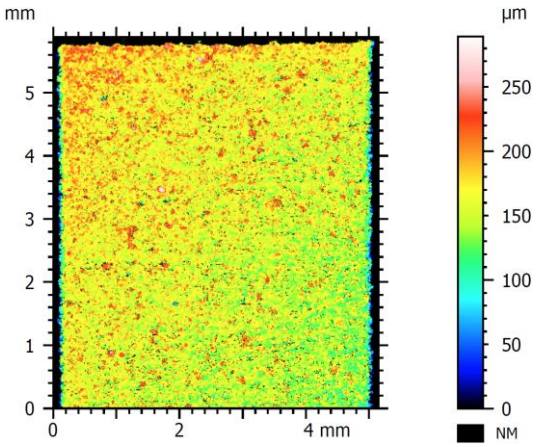

Figure 4. SW surface of sample 60 scanned using a 10x objective and 0.5x tube lens. "NM" indicates non-measured points.

Additionally, each surface was scanned over a 3 x 3 stitch using a 20x objective and 1.0x tube lens to create an 895 µm x 895 µm view of the surface with 0.312 µm point spacing. The scan center was positioned at (2.5,-3) mm assuming the upper left corner of the surface is (0,0). An example data set, leveled and outliers removed using the commercially available ConfoMap software, can be seen in Figure 5.

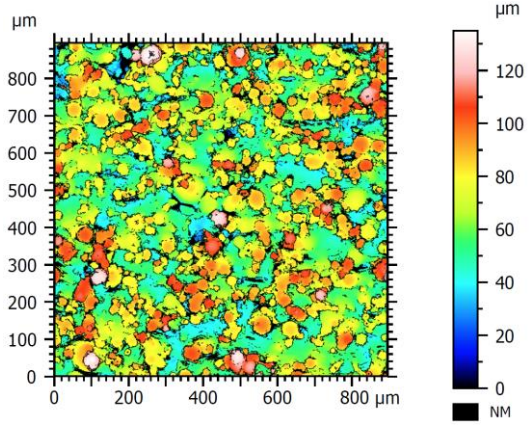

Figure 5. SW surface of sample 60 scanned using a 20x objective. Center of the scan is positioned at (2.5,-3) mm assuming the upper left corner of the surface (seen in Figure 4) is the position (0,0).

3.2. Analysis of XCT data

The reconstructed XCT data were imported into VGStudioMAX 3.0 software and the 3-2-1 registration technique available in the software was used to align the orthogonal faces to the same coordinate system and minimize part-to-part variation during the analysis [16]. Then, a stack of images was exported such that the cross-sectional image shows both SW and NE edges of the sample. The XCT data set can be also converted to a mesh after the surface is determined from XCT grayscale images. The software provides an advanced local adaptive surface detection algorithm which can determine the surface at a sub-voxel level [16]. Lifton et al. [17] estimated the uncertainty of dimensional measurement based on a similar surface detection method to be at sub-pixel level in case of a 2D image. The determined surface can be exported to an STL file for a comparison with other measurement results. Example surface representations are shown in Figure 6.

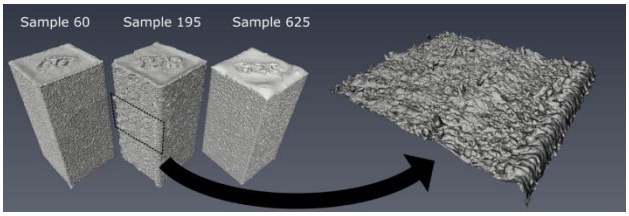

Figure 6. Example XCT-based surface representations of different AM processing parameters

For the initial characterization, full resolution grayscale XCT images representing cross sections of the samples were converted to binary using a 50 % digital level threshold instead of using the more complex sub voxel interpolated surfaces. The sub voxel interpolated surfaces will be used for the future analysis. The uncertainty of the current surface detection is estimated to be at around a voxel level, but a more comprehensive simulation study would improve the estimation. The binary images are then converted to a "top down" measurement, analogous to how an optical metrology system would obscure the underside of overhangs. This is accomplished by searching through each column of pixels to determine the point at which the image data changes from a value of zero to a value of one. Figure 7 shows examples of the XCT image, binary threshold, and resultant profile highlighted in red.

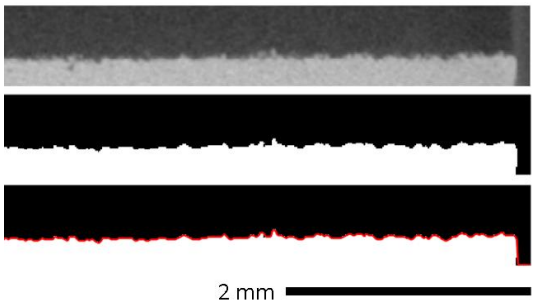

Figure 7. XCT data (top), converted to binary (middle), with conversion to surface profile (bottom).

Using this method, a 2D array of surface heights can be created and imported into the same commercially available software used to analyse data from the laser confocal system. An example of this data can be seen in Figure 8.

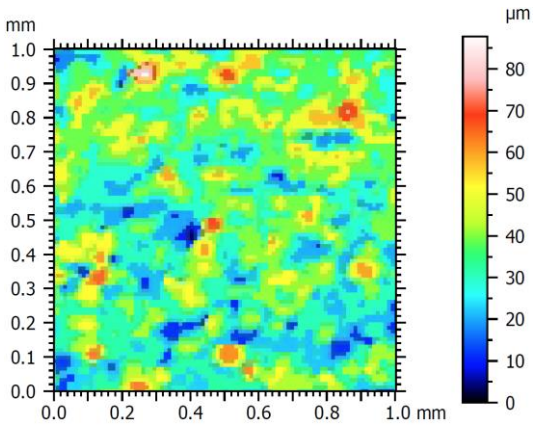

Figure 8. SW surface of sample 60 derived from XCT data. This region is the same general area scanned by the laser confocal system using the 20x objective (Figure 5).

Although prominent particles can be visually identified, the current resolution prevents significant statistical analysis of the XCT data. However, higher resolution scans of the samples are currently underway.

4. Comparison of Results

Images of the surface were taken via scanning electron microscope (SEM) for qualitative comparison. Figure 9 shows an example image from the SW surface of sample 60. The image shows a 1 mm x 1 mm area of the surface that encompasses the area previously scanned with the laser confocal microscope using the 20x objective (Figure 5).

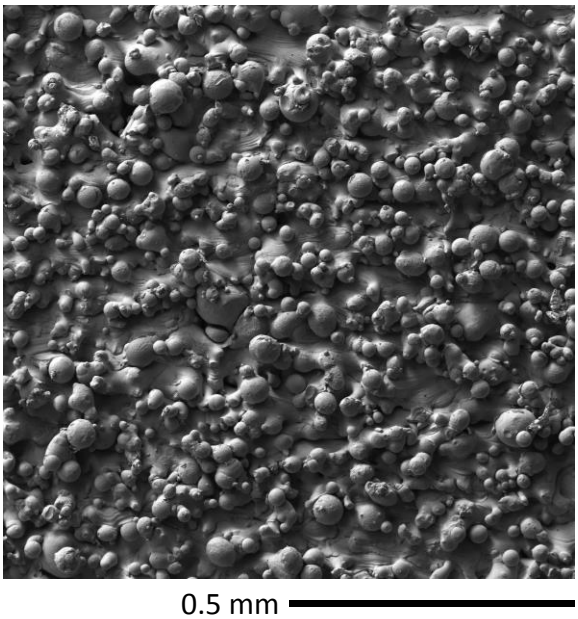

Figure 9. SW surface of sample 60 taken via SEM. Image is a 1 mm x 1 mm area that encompasses the laser confocal data scanned using the 20x objective (Figure 5).

While the current resolution of the XCT data is limited, it has the distinct advantage of being able to detect pores and undercuts on and near the surface. To detect pores and undercuts, the binary images were used to create a profile in a similar fashion as described in section 3.1. However, instead of the "top down" approach, the profile is determined from approximately 500 µm below the surface to the surface. This "bottom up" profile is then compared to the "top down" profile and any variations between the two profiles are tracked as pores and undercuts. An example of this methodology is presented in Figure 10 and the resultant pore and undercut locations are presented in Figure 11.

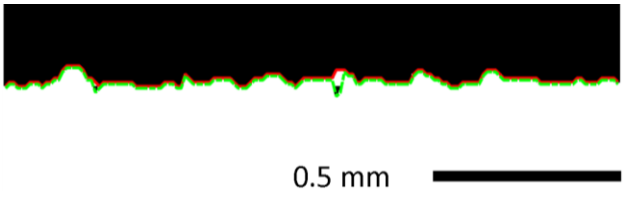

Figure 10. Example of "top down" (red) and "bottom up" (green) profiles for tracking pores and undercuts.

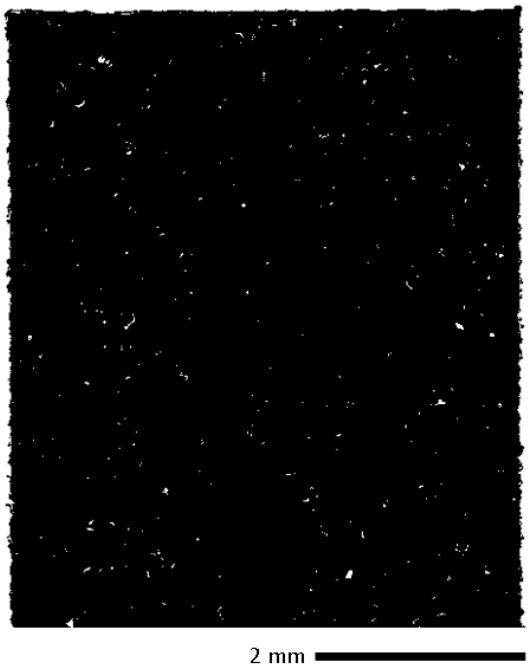

Figure 11. Identification of near surface pores and undercuts on the SW surface of sample 60 using XCT data.

From the identification of pores and undercuts in Figure 11, surface data near these defects can be extracted. The XCT data and surface data taken with the 20x objective were aligned manually by visually aligning prominent features in the false color height maps from Figure 5 and Figure 8 using commercially available image processing software. Pore locations are highlighted in Figure 12. A closer view of the surface data near the defect location in the upper left corner of Figure 12 is shown in Figure 13. While this methodology allows us to align and identify regions where subsurface defects exist, it is still inconclusive if trends in the surface data from the laser confocal system can identify these defects. As such, further analysis of the surface data is ongoing.

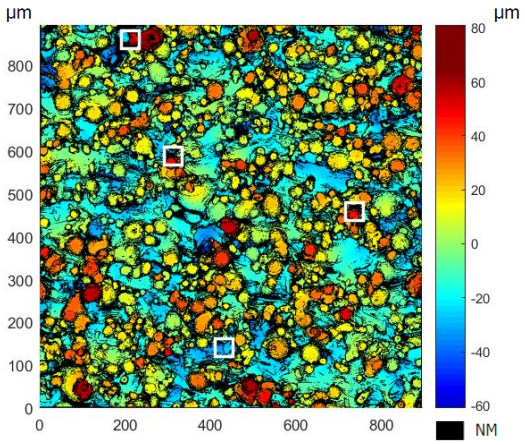

Figure 12. Surface data for the SW surface of sample 60, taken via 20x objective on the laser confocal system, with defect areas (pore and undercut locations) highlighted by white boxes.

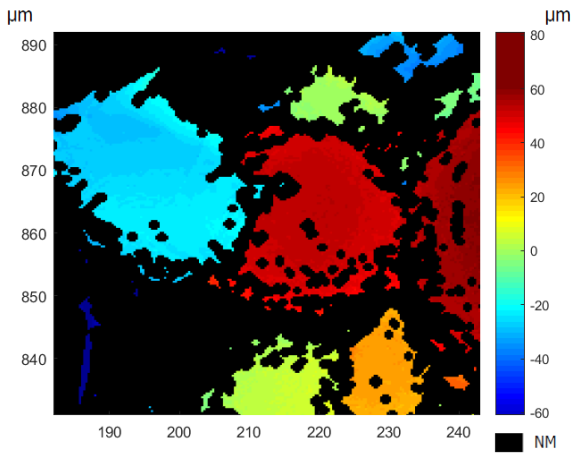

Figure 13. Surface data taken via 20x objective on the laser confocal microscope for the upper left defect area from Figure 12.

5. Conclusions

In this work, IN625 and 17-4SS samples were built on a commercially available L-PBF system and analyzed via laser confocal microscope and XCT. The data was then manually aligned for complementary analysis. Pores and undercuts were identified using XCT data, which allowed for more stringent analysis of the surface near these features. However, at 10.9 µm/voxel the current resolution of XCT prevents strong quantitative analysis of the surface data from XCT or relevant comparison to the laser confocal microscope surface data. To resolve this issue, higher resolution XCT scans at an anticipated resolution of ≈2 µm/voxel are currently underway. Additionally, the higher resolution will allow for identification of smaller pores and undercuts. While quantitative analysis has been performed on XCT data with larger voxel resolutions, it has required the use of sub-voxel interpolation, which is currently not included in this analysis. Additionally, the work has focused on top surfaces as opposed to side surfaces of the AM parts, which generally contain larger scaled surface features and ease resolution requirements for a strong quantitative analysis. With an increased focus on quantitative analysis forthcoming, an investigation of uncertainty will be required and is planned for future work.

Future work will also include the classification of defects found in the data (i.e., subsurface pores vs undercuts on the surface), and identification of the depth of pores. Additionally, advanced pore detection techniques and image analysis, such as those presented in Kim et al. [18], automated alignment techniques, such as those presented in Thompson et al. [11], and sectioning of the samples for comparison to the XCT and laser confocal microscope data are in progress. It is anticipated that this type of analysis will create avenues to get richer information from the surface data and add a potential methodology for feature based metrology.

6. Acknowledgements

This work was performed in part in the NIST Center for Nanoscale Science and Technology (CNST) Nanofab Facility.

References

[1] NIST, US Department of Commerce 2012 Measurement Science Roadmap for Metal-Based Additive Manufacturing. Gaithersburg, MD.

[2] Yadroitsev I 2009 Selective laser melting: direct manufacturing of 3D-objects by selective laser melting of metal powders *Saarbrücken* (Lambert Acad. Publ)

[3] Pyka G, Burakowski A, Kerckhofs G, Moesen M, Van Bael S, Schrooten J 2012 Surface modification of Ti6Al4V open porous structures produced by additive manufacturing *Adv. Eng. Mat.* **14** 363–70

[4] Townsend A, Senin N, Blunt L, Leach R, Taylor J S 2016 Surface texture metrology for metal additive manufacturing: a review *Precision Engineering* **46** 34–47

[5] Fox J C, Moylan S P, Lane B M 2016 Preliminary Study Toward Surface Texture as a Process Signature in Laser Powder Bed Fusion Additive Manufacturing. *Proceedings of the 2016 ASPE Summer Topical Meeting: Dimensional Accuracy and Surface Finish in Additive Manufacturing*, Raleigh, NC

[6] Fox J C, Moylan S P, Lane B M 2016 Effect of Process Parameters on the Surface Roughness of Overhanging Structures in Laser Powder Bed Fusion Additive Manufacturing *Procedia CIR*P **45** 131–4

[7] Thompson A, Maskery I, Leach R 2016 X-ray computed tomography for additive manufacturing: a review *Meas Sci Technol* **27** 072001

[8] Kerckhofs G, Pyka G, Moesen M, Van Bael S, Schrooten J, Wevers M 2013 High-Resolution Microfocus X-Ray Computed Tomography for 3D Surface Roughness Measurements of Additive Manufactured Porous Materials *Adv. Eng. Mater.* **15** 153–8

[9] Townsend A, Pagani L, Scott P, Blunt L 2017 Areal surface texture data extraction from X-ray computed tomography reconstructions of metal additively manufactured parts *Precision Engineering* **48** 254–64

[10] Thompson A, Körner L, Senin N, Lawes S, Maskery I, Leach R 2017 Measurement of internal surfaces of additively manufactured parts by X-ray computed tomography. *7th Conference on Industrial Computed Tomograph*y Leuven, Belgium

[11] Thompson A, Senin N, Giusca C, Leach R 2017 Topography of selectively laser melted surfaces: A comparison of different measurement methods *CIRP Annals - Manufac. Technol.* **66(1)** 543-6

[12] Hernandez A M, Boone J M 2014 Tungsten anode spectral model using interpolating cubic splines: Unfiltered x-ray spectra from 20 kV to 640 kV *Med Phys* **41** 042101

[13] Feldkamp L A, Davis L C, Kress J W 1984 Practical cone-beam algorithm *J. Opt. Soc. Am. A* **1(6)** 612-9

[14] Material data sheet - EOS StainlessSteel GP1 for EOSINT M270 2009. https://scrivito-public-cdn.s3-eu-west-1.amazonaws.com/eos/public/5f84f5d2c88ac900/05fb1582834a38c85ef6dd859733a230/EOS_StainlessSteel-GP1_en.pdf (accessed December 7, 2015).

[15] Material Data Sheet - EOS NickelAlloy IN625 2011. http://ip-saas-eos-cms.s3.amazonaws.com/public/d1327facdca0e32a/373a60ec4f5c891b7dbcdf572e37d3b0/EOS_NickelAlloy_IN625_en.pdf (accessed June 13, 2017).

[16] Volume Graphics GmbH, VGStudioMax 3.0.

[17] Lifton J J, Malcolm A A, McBride J W 2015 On the uncertainty of surface determination in x-ray computed tomography for dimensional metrology *Meas. Sci. Technol.* **26** 035003

[18] Kim F H, Garboczi E J, Moylan S P, Slotwinski J A 2017 Investigation of pore structure in cobalt chrome additively manufactured parts using X-ray computed tomography and three-dimensional image analysis *Additive Manufacturing* **17** 23-38